AIAA JOURNAL
Vol. 41, No. 11, November 2003

Prediction of Nonlinear Behavior of Composites via Micromechanics Using Matrix Bulk Properties

Virendra R. Jadhav*
Endicott Interconnect Technologies, Endicott, New York 13760
and
Srinivasan Sridharan†
Washington University in St. Louis, St. Louis, Missouri 63130

Prediction of nonlinear response of laminated composite structural elements is attempted using the actual bulk properties of the matrix instead of the modified in situ properties that are determined to fit experimental results of a lamina. Two competing micromodels, namely, a simplified square cells model (SSCM) and a finite element-based cylindrical model (FECM), are used in the investigation. Residual stresses in the matrix due to thermal curing, shear softening, and microcracking are all explicitly accounted for. Alternative ways of treating microcracking are presented. Comparisons of the analytical predictions and experimental observations for a V-notched beam specimen and axially compressed 45/−45 deg carbon–epoxy cylindrical shells are presented. In both cases it was found that the FECM combined with a coupled crack option provides a consistent estimate of the experimental response. The SSCM, however, does not fare well in comparison.

Nomenclature

$d\varepsilon_{ij}^{c}$	=	increments in matrix strain component with respect to axes oriented along crack plane
$d\varepsilon_{i}^{k}$	=	increment in in-plane strain in the kth layer of a laminate
$d\varepsilon_{o}^{k}$	=	increment in out-of-plane strains in the kth layer of a laminate
$d\sigma_{ij}^{c}$	=	increments in matrix stress component with respect to axes oriented along crack plane
$d\sigma_{i}^{k}$	=	increment in in-of-plane stresses in the kth layer of a laminate
$d\sigma_{o}^{k}$	=	increment in out-in-plane stresses in the kth layer of a laminate
E	=	Young's modulus of the epoxy
E_1	=	longitudinal Young's modulus of the fibers
E_2	=	transverse Young's modulus of the fibers
F	=	appropriately chosen large positive value
G_{12}	=	longitudinal shear modulus of the fibers
G_{23}	=	transverse shear modulus of the fibers
$[P^k]$	=	partially inverted stiffness matrix of the kth layer of a laminate
S_{ij}	=	deviatoric stress, compliance matrix components
V_f	=	fiber volume content
$\alpha_1, \alpha_2, \alpha_m$	=	coefficient of thermal expansion of the fiber in longitudinal direction, transverse direction, and matrix
δ_{ij}	=	Kronecker delta, 1 or 0, for $i = j$ and $i \neq j$, respectively
ν	=	Poisson's ratio of the epoxy
σ_{eq}	=	equivalent stress
σ_o, n	=	Ramberg–Osgood material parameters of the epoxy
σ_T	=	total residual stress field in the representative volume element (RVE)
σ_T^1	=	residual stress field in the RVE due to curing for a single lamina.
σ_T^2	=	residual stress field in the RVE due to curing arising from different fiber orientations in a laminate
σ_{ult}	=	matrix failure stress in unidirectional tension

Received 11 November 2002; revision received 20 May 2003; accepted for publication 2 June 2003.

*Stress Analyst, Reliability and Simulation.
†Professor, Department of Civil Engineering. Senior Member AIAA.

Introduction

A MICROMECHANICAL model determines the thermomechanical properties of a composite material from the knowledge of the thermomechanical properties of its constituents and their relative proportions. When a material is to be optimized for a specific application, a micromechanical model can provide useful information via simulations and eliminate costly parametric experimental studies.

Micromechanical analysis involves representing a lamina by a cell consisting of volumes of constituent materials arranged in a specific way, so that the behavior of the cell in average describes that of the lamina. Such a cell is called the representative volume element (RVE). The value of fiber volume fraction of the lamina, V_f, is maintained in the RVE. In the case of unidirectional long fiber composites, the high ratio of the length of the fiber to its diameter makes it possible to treat the micromechanical response of the RVE as a generalized plane strain problem, that is, with constant strains in the fiber direction.

Most micromechanical models for long fiber composites can be classified into two broad categories: 1) models based on a square-cells-type RVE, for example, the method of cells[1] and the free transverse shear approach[2] and 2) models based on a circular-cells-type RVE, for example, Hill's self-consistent model[3] and Hashin and Rosen's composite cylinder models.[4] An extensive survey of these models is available in literature.[5–9]

The most frequently used micromodels for studying the nonlinear material effects are those based on RVE in the form of a square cell mainly because of their simplicity and numerical efficiency. Aboudi[1,10] and Arenberg[11] have illustrated the use of method of cells for nonlinear applications, such as nonlinear elastic matrix, elastoplastic matrix, viscoplastic matrix, etc. Robertson and Mall[12,13] have used the free transverse shear approach to deal with viscoplasticity of matrix, effects of fiber–matrix interface, as well as fiber damage for metal matrix composites. Nonlinear response of polymer matrix composites was predicted by Gates et al.[14] using Sun and Chen's square cell model.[15] Pecknold and Haj Ali[16] and Pecknold and Rahman[17] have performed nonlinear analysis of composites

using a simplified version of the square-cells-type micromechanical model. All of these studies make use of the in situ properties of the matrix, backed out from tests on the composite laminas. In-plane shear response of the composite material is first determined experimentally. The nonlinear parameters of the material model (typically a shear-softening model) used to characterize the matrix are then so determined that the predictions of the micromechanical analysis agrees with the experimental in-plane shear response of a lamina. This approach though seemingly successful has some drawbacks. The nonlinear parameters of the matrix determined in this approach are not real properties; they are specific to the fiber volume fraction of the tested lamina and have been tuned to compensate for the deficiency of the RVE of the model in describing the composite, matrix cracking, and the presence of residual stresses. It appears reasonable to take the view that micromechanical models must be based as much as possible on the actual properties of the constituent materials, that is, fibers and matrix, rather than parameters obtained from fitting their response to one set of experimental results of a lamina. The models will then be transparent and reveal more fully the phenomena investigated. They will also be more versatile because they can then be confidently extended to phenomena not studied so far. The approach taken in this study is based on this premise.

The authors have investigated a representative model from each of the two broad classes, namely, the simplified square cells model (SSCM) and the finite element-based cylindrical model (FECM). The effect of using bulk properties of the matrix in these micromechanical models was investigated by the authors.[18,19] The earlier work indicated that, in the approach the authors were taking, the inclusion of residual stresses and matrix microcracking is critical to prediction of nonlinear response of a composite laminate, whereas, in the case of laminas under off-axis tension, failure occurs before their effects could be clearly discernible. This has provided the motivation to continue the study further into laminates and composite structural elements using the present approach.

For completeness, a brief review of the overall analysis scheme including the sublaminate models and the generic details of the micromodels (such as matrix softening models and smeared crack models) and specifics of the two micromodels employed, namely, FECM and SSCM , are presented. This is followed by a presentation of the results of the two case studies.

Overall Analysis Scheme and Components

The present scheme of nonlinear analysis of composite materials involves the calculations at the lamina level, the sublaminate level, and the structural level.

Lamina Level

Micromodels are employed to perform a dual role: 1) They are tools for homogenizing the composite lamina, given the current properties of the matrix and fibers. 2) They perform the role of computing the stresses and strains in the fibers and the matrix, given those in the composite lamina. Fibers are assumed to be linearly elastic, whereas the matrix is characterized by a softening law and a failure criterion to signal cracking. Residual stresses due to curing are also to be computed at the start of the analysis. This stress field in matrix is denoted as σ_T^1.

In the determination of the thermal residual stresses in the matrix, the properties of the fiber and the matrix are treated as linear elastic. Variations of mechanical and thermal properties with temperature are not considered in this study.

Laminate Level

The second step in determination of material properties involves computing properties of the laminate created by stacking several laminas with differing orientations. When stress gradients across the thickness of a laminate are to be accounted for, it is necessary to introduce numerical integration points across the thickness of the laminate in finite element analyses. The representative material properties at the integration point are derived from the sublaminate model installed at the point. Sublaminate models perform a dual role: 1) They are the tools for local homogenization, that is, of computing stress–strain relations of the composite laminate for the tributary area allocated to them. 2) They are used to compute the stresses and strain in each of the laminas in the tributary area, given the composite stresses and strains prevailing in the tributary area.

Often, considerable simplification is possible in composite laminates made up of a large number of laminas arranged in a repeating stacking sequence. (We shall call such a repeating sequence the ply unit.) The local material properties, for example, tangential stress–strain relations, of a laminate at a certain integration station point across the thickness are typified by the ply unit, and it is necessary and sufficient to consider just one ply unit installed at the integration point to characterize the entire tributary area.

Because of the different orientations of individual laminas in a sublaminate, residual stresses develop in the laminas during curing. These stresses give rise to an additional field of residual microstresses σ_T^2 in the matrix. The total residual stresses in matrix are, then, $\sigma_T = \sigma_T^1 + \sigma_T^2$. When stress gradients across the thickness of a laminate are to be accounted for, it is necessary to introduce numerical integration points across the thickness of the laminate in finite element analyses. Thus, the variation of material properties in the thickness direction of the laminate are accounted for.

Thus, the analysis is done using following steps (Fig. 1):

1) The initial thermomechanical properties of a single lamina are obtained via a micromodel. Also the initial stress field due to thermal curing, σ_T^1, in the matrix is obtained.

2) Properties of the sublaminate are determined from the sublaminate model at every integration point. From this, thermal residual stresses at each lamina are determined. When the micromechanical model for laminas, σ_T^2, is used, the additional field of thermal residual stresses in the matrix is obtained and is superimposed on σ_T^1, to get the total residual stresses in matrix, $\sigma_T = \sigma_T^1 + \sigma_T^2$.

3) Properties of the matrix are updated to account for the residual stresses, and the micromodel and sublaminate model are called again to get the correct initial properties of the homogenized composite.

4) The homogenized sublaminate properties are provided for all integration points for all finite elements. With knowledge of the geometric and material data, the structural stiffness matrix is set up.

5) A load increment is applied. Finite element equations are solved to get the basic variables (displacements and rotations).

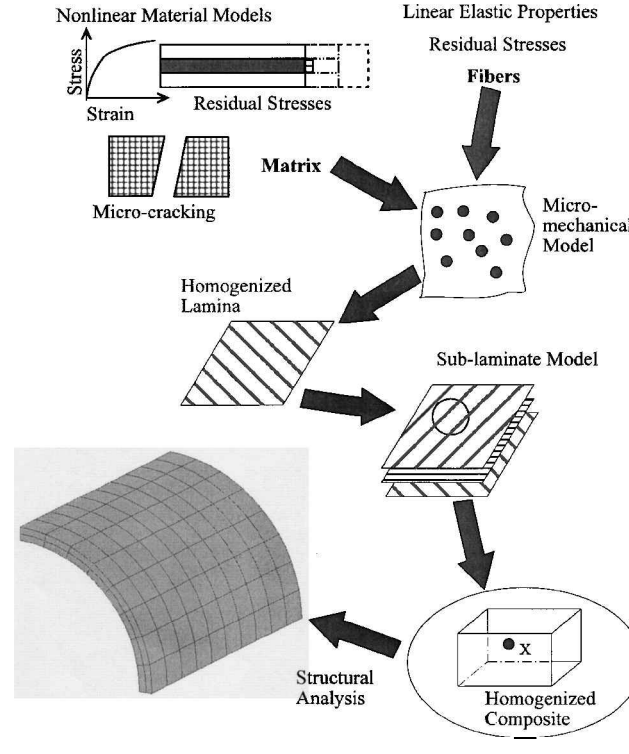

Fig. 1 Overall scheme for micromechanics-based analysis.

Stresses and strains at various integration points in all of the elements are obtained.

6) For each element, and for each integration point in it, the sublaminate model is called to distribute the stresses and strains among several laminas that make up the sublaminate.

7) For each lamina in the sublaminate, the micromechanical model is called to get the stress and strain increments in the matrix and fiber.

8) Matrix properties are updated using a nonlinear material model. Checks are performed to detect microcracking using a valid failure theory for matrix failure. Matrix properties are adjusted for cracking, if it occurs.

9) Updated matrix properties are combined with fiber properties via the micromechanical model to get updated properties of the homogenized lamina.

10) Updated properties of all of the laminas in a sublaminate are passed to the sublaminate model to determine the updated properties of the homogenized composite.

11) Steps 4–10 are repeated until desired loading level is reached.

The implementation of this scheme was done in conjunction with commercial code ABAQUS[20] through user subroutine UMAT. Different modules of the overall analysis scheme are described in brief in the following sections.

Sublaminate Model

Pecknold's sublaminate model (see Refs. 16 and 17) used in this study is based on the following assumptions, which ensure equilibrium and compatibility at the sublaminate level:

1) Out-of-plane stresses are continuous between adjacent laminas.

2) In-plane strains are continuous between adjacent laminas.

3) Stresses and strains are constant across the thickness of a lamina.

4) Stresses and strains acting on the homogenized sublaminate are volume averages of the stresses and strains of individual laminas.

From the current tangential stress–strain relations of a lamina, for example, the kth, of the ply unit, the increments of the discontinuous quantities can be related to the conjugate continuous quantities in terms of a $[P^k]$ matrix of the lamina as

$$\begin{Bmatrix} d\sigma_i^k \\ d\varepsilon_o^k \end{Bmatrix} = \begin{bmatrix} P_{ii}^k & P_{io}^k \\ P_{oi}^k & P_{oo}^k \end{bmatrix} \begin{Bmatrix} d\varepsilon_i^k \\ d\sigma_o^k \end{Bmatrix} \tag{1}$$

where the subscripts i and o stand for the in-plane and the out-of-plane quantities, respectively.

Over the ply unit, in-plane strains $d\varepsilon_i$ and out-of-plane stresses $d\sigma_o$ are considered constant, so that by summation of these equations over all of the laminas, a relationship similar to Eq. (1) for the entire ply unit can be obtained in terms of a $[\bar{P}]$ matrix:

$$\begin{Bmatrix} d\bar{\sigma}_i \\ d\bar{\varepsilon}_o \end{Bmatrix} = \begin{bmatrix} \bar{P}_{ii}^k & \bar{P}_{io}^k \\ \bar{P}_{oi}^k & \bar{P}_{oo}^k \end{bmatrix} \begin{Bmatrix} d\varepsilon_i \\ d\sigma_o \end{Bmatrix} \tag{2}$$

where

$$[\bar{P}] = \frac{1}{t} \sum t_k [P^k]$$

and t_k and t are the thicknesses of the kth lamina and the entire ply unit, respectively. The $[\bar{P}]$ matrix can be partially inverted to obtain the stiffness matrix required in the analysis. More details of the model may be found elsewhere.[8,21]

Matrix Modeling: Nonlinear Response and Microcracking

The principal source of nonlinearity in the matrix response is shear softening. A nonlinear behavior can be described by a generalized Ramberg–Osgood material model under static, monotonic loading, which was of interest in the present study. The total stress-total strain (tensorial) relations for the Ramberg–Osgood model are given by (see Ref. 1)

$$\varepsilon_{ij} = [(1+\nu)/E]\sigma_{ij} - (\nu/E)\sigma_{kk}\delta_{ij} + (3/2E)S_{ij}(\sigma_{\text{eq}}/\sigma_o)^{n-1} \tag{3}$$

where $S_{ij} = \sigma_{ij} - \frac{1}{3}\sigma_{kk}\delta_{ij}$ is deviatoric stress and $\sigma_{\text{eq}} = \sqrt{(\frac{3}{2}S_{ij}S_{ij})}$ is equivalent stress.

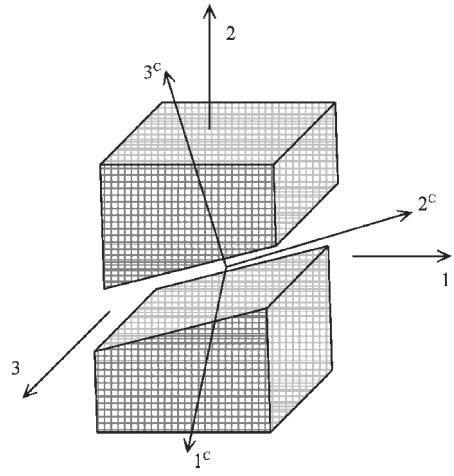

Fig. 2 Matrix microcracking.

As a lamina is loaded, several microcracks develop in the matrix. The multiplicity of such cracks and the lack of a physical scale in the representative volume element approach make it unreasonable to deal with such cracks through a fracture mechanics approach. Instead, an approach used successfully in reinforced concrete is used in the current research. This is called the smeared crack approach.[22] The smeared crack approach uses a failure criterion to signal crack initiation and then selectively degrades the stiffness of the matrix. Maximum principal stress theory was used to predict failure and crack initiation. Thus, if the maximum tensile principal stress in matrix exceeds the matrix failure stress in unidirectional tension, σ_{ult}, a crack is introduced in the perpendicular direction. (Note that cracks can initiate at different locations in the RVE representing a lamina.)

The tangential stress–strain relations of the matrix referred to the principal axes of stress (Fig. 2) at a typical location in the micromodel after some shear softening but before cracking take the form

$$\begin{Bmatrix} d\varepsilon_{11}^c \\ d\varepsilon_{22}^c \\ d\varepsilon_{33}^c \\ d\gamma_{23}^c \\ d\gamma_{31}^c \\ d\gamma_{12}^c \end{Bmatrix} = \begin{bmatrix} S_{11}^c & S_{12}^c & S_{13}^c & S_{14}^c & S_{15}^c & S_{16}^c \\ S_{21}^c & S_{22}^c & S_{23}^c & S_{24}^c & S_{25}^c & S_{26}^c \\ S_{31}^c & S_{32}^c & S_{33}^c & S_{34}^c & S_{35}^c & S_{36}^c \\ S_{41}^c & S_{42}^c & S_{43}^c & S_{44}^c & S_{45}^c & S_{46}^c \\ S_{51}^c & S_{52}^c & S_{53}^c & S_{54}^c & S_{55}^c & S_{56}^c \\ S_{61}^c & S_{62}^c & S_{63}^c & S_{64}^c & S_{65}^c & S_{66}^c \end{bmatrix} \begin{Bmatrix} d\sigma_{11}^c \\ d\sigma_{22}^c \\ d\sigma_{33}^c \\ d\sigma_{23}^c \\ d\sigma_{31}^c \\ d\sigma_{12}^c \end{Bmatrix} \tag{4}$$

where it is understood that $S_{ij}^c = S_{ji}^c$ and the 3^C axis is normal to the plane of maximum principal stress.

In the present study, four alternative ways of selectively degrading the matrix stiffness were employed.[19,21] They are described briefly as follows:

1) In the no cracking option, microcracking is ignored. This is the highest bound on the stress–strain response.

2) In the uncoupled cracking option, it is assumed that a) once a crack occurs, the material is incapable of communicating normal and shear stresses across the crack, that is $d\sigma_{33}^c = d\sigma_{23}^c = d\sigma_{13}^c = \delta$, where $\delta \to 0$, and b) the incremental strain components across the crack plane, $d\varepsilon_{33}^c$, $d\gamma_{23}^c$, and $d\gamma_{13}^c$, are not coupled in any way to incremental stress components in the 1^c–2^c plane, namely, $d\sigma_{11}^c$, $d\sigma_{22}^c$, and $d\sigma_{12}^c$. Thus, we set

$$\begin{Bmatrix} d\varepsilon_{11}^c \\ d\varepsilon_{22}^c \\ d\varepsilon_{33}^c \\ d\gamma_{23}^c \\ d\gamma_{31}^c \\ d\gamma_{12}^c \end{Bmatrix} = \begin{bmatrix} S_{11}^c & S_{12}^c & 0 & 0 & 0 & S_{16}^c \\ S_{21}^c & S_{22}^c & 0 & 0 & 0 & S_{26}^c \\ 0 & 0 & F \cdot S_{33}^c & 0 & 0 & 0 \\ 0 & 0 & 0 & F \cdot S_{44}^c & 0 & 0 \\ 0 & 0 & 0 & 0 & F \cdot S_{55}^c & 0 \\ S_{61}^c & S_{62}^c & 0 & 0 & 0 & S_{66}^c \end{bmatrix} \begin{Bmatrix} d\sigma_{11}^c \\ d\sigma_{22}^c \\ d\sigma_{33}^c \\ d\sigma_{23}^c \\ d\sigma_{31}^c \\ d\sigma_{12}^c \end{Bmatrix} \tag{5}$$

where F is an appropriately chosen large positive value. This postulation leaves the crack strains unaffected by the actions in plane 1^c–2^c. It simply blocks one path for the flow of stresses. Furthermore, there is full mutual decoupling of the strains associated with the x_3 direction. Obviously this formulation does not account for the complex stress redistribution associated with the formation of a crack and the local damage that follows.

3) With the coupled cracking option, the incremental stresses are, once again, maintained at zero, $d\sigma^c_{33} = d\sigma^c_{23} = d\sigma^c_{13} = \delta$, with $(\delta \to 0)$. In this case, however, the incremental stresses in 1^c–2^c plane interact with incremental strains $d\varepsilon^c_{33}$, $d\gamma^c_{23}$, and $d\gamma^c_{13}$. In addition, there is full mutual interaction between the strains and stresses associated with the 3^c direction. The nature of the interaction is such that none of the stresses can increase in the same sense as that obtained before cracking without causing rapid crack growth. Because the strains on the crack plane cannot increase without reference to the strains in the neighboring points, the pattern of stress evolution obtained before crack nucleation is disrupted. Thus, in this option, we set

$$\begin{Bmatrix} d\varepsilon^c_{11} \\ d\varepsilon^c_{22} \\ d\varepsilon^c_{33} \\ d\gamma^c_{23} \\ d\gamma^c_{31} \\ d\gamma^c_{12} \end{Bmatrix} = \begin{bmatrix} S^c_{11} & S^c_{12} & F\cdot S^c_{13} & F\cdot S^c_{14} & F\cdot S^c_{15} & S^c_{16} \\ S^c_{21} & S^c_{22} & F\cdot S^c_{23} & F\cdot S^c_{24} & F\cdot S^c_{25} & S^c_{26} \\ F\cdot S^c_{31} & F\cdot S^c_{32} & F\cdot S^c_{33} & F\cdot S^c_{34} & F\cdot S^c_{35} & F\cdot S^c_{36} \\ F\cdot S^c_{41} & F\cdot S^c_{42} & F\cdot S^c_{43} & F\cdot S^c_{44} & F\cdot S^c_{45} & F\cdot S^c_{46} \\ F\cdot S^c_{51} & F\cdot S^c_{52} & F\cdot S^c_{53} & F\cdot S^c_{54} & F\cdot S^c_{55} & F\cdot S^c_{56} \\ S^c_{61} & S^c_{62} & F\cdot S^c_{63} & F\cdot S^c_{64} & F\cdot S^c_{65} & S^c_{66} \end{bmatrix} \times \begin{Bmatrix} d\sigma^c_{11} \\ d\sigma^c_{22} \\ d\sigma^c_{33} \\ d\sigma^c_{23} \\ d\sigma^c_{31} \\ d\sigma^c_{12} \end{Bmatrix} \tag{6}$$

where F is an appropriately chosen large number.

4) In the full cracking option, all of the six diagonal elements of the compliance matrix are made arbitrarily high numbers, and all of the off diagonal elements are made zero. This option is the lowest bound on the stress–strain response.

In principle, one must set F to be an arbitrarily large value to ensure vanishingly small increments of stress across the crack. However, this could make the $[S]$ matrix highly ill conditioned and noninvertible. The authors recommend a value of 100 (a 100-fold increase in compliance) based on numerical experiments.

Micromechanical Models

Two competing micromechanical models were studied: SSCM and FECM. Each of them represents a class of models popularly used in literature. Effects of the interface and interphase regions are neglected, and a perfect bond between fibers and matrix was assumed.

SSCM

In the SCCM, the composite is assumed to consist of a doubly periodic array of square fibers, with equal spacing in the two transverse directions $X2$ and $X3$. A representative volume then consists of four subcells, one of fiber (11) and three of matrix (12, 21, 22), as shown in Fig. 3. The model is based on the following mechanics of materials assumptions, which ensure overall equilibrium and compatibility of the RVE:

1) Stresses and strains are constants over each subcell.

2) The axial strain in all the subcells is the same as the axial strain in the homogenized lamina.

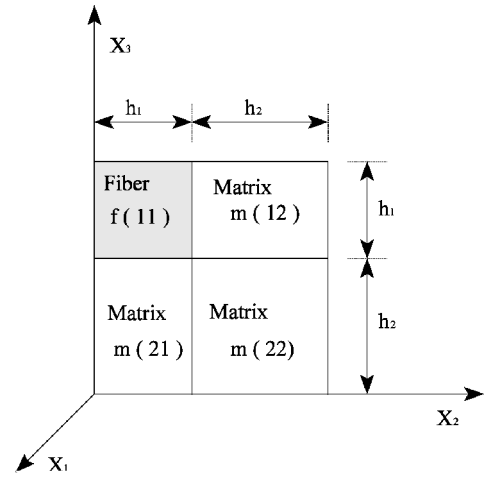

Fig. 3 SSCM.

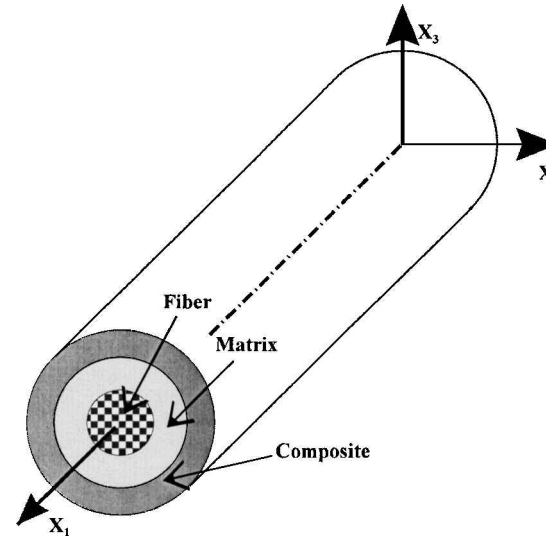

Fig. 4 FECM.

3) Fiber subcell (11) and matrix subcell (12) carry the same stress in the two direction. Similarly, the matrix subcells (21) and (22) carry the same stress in the two direction. Furthermore, the total strain in the two direction in subcells (11) and (12) combined is the same as the total strain in the two direction in subcells (21) and (22) combined.

4) Fiber subcell (11) and matrix subcell (21) carry the same stress in the three direction. Similarly the matrix subcells (12) and (22) carry the same stress in the three direction. Furthermore, the total strain in the three direction in subcells (11) and (21) combined is the same as the total strain in the three direction in subcells (12) and (22) combined.

5) The transverse shear stress in all of the subcells is the same as the transverse shear stress in the homogenized lamina.

A set of simultaneous equations is set up based on these postulations to relate the stresses, strains, and stiffnesses of the homogenized lamina to the stresses, strains, and stiffnesses of the individual subcells of the RVE that represents the lamina. The residual stresses are obtained from the same governing equations, by setting the imposed composite stresses to be zero (see Appendix of Ref. 19).

FECM

The FECM treats the composite material as a random array of circular fibers. The representative volume element consists of a composite-cylinder-type assemblage as shown in Fig. 4. The model is made up of three zones, representing the fiber, the matrix, and the composite. The outer elements are annular, and for simplicity the

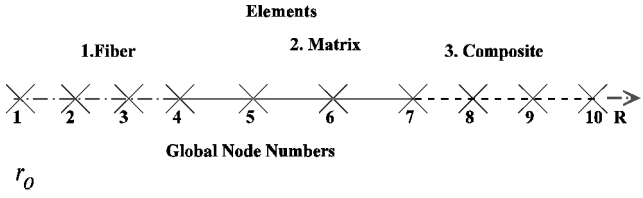

Fig. 5 FECM discretization.

fiber element, too, is treated as annular. The homogenized stresses and strains over the lamina are the volumetric averages of the stresses and strains over the combined constituent fiber and matrix phase volumes V only.

The compliance of the composite is obtained by applying unit values of the six stress components over the model, that is, $\bar{\sigma}^{\text{app},i} = 1$, $i = 1, \ldots, 6$. In each case, the averaged strains $\bar{\varepsilon}^i_j$, $j = 1, \ldots, 6$ over V are determined. This gives the compliance matrix $\bar{S}_{jk}$. The solution of these problems can likewise give the stress distributions in matrix and fiber.

These problems are solved using finite ring elements. The ratio of the radii of the fiber element to the outer radius of the matrix element is determined from the fiber volume fraction. The outer radius of the composite element must be sufficiently large, but otherwise can be arbitrary.[18]

The strain–displacement relations in cylindrical polar coordinates $(r - \theta)$ based on linear three-dimensional elasticity are employed. The following are the features of the model:

1) The strains are assumed constant in the fiber direction.

2) In the circumferential θ direction, the shape functions take the form of selected Fourier harmonics. Numerical integration is employed taking at least 12 integration points in the θ direction to account for the variation of matrix properties.

3) In the radial r direction, shape functions take the form of cubic polynomials (Fig. 5). Given the higher-order nature of the shape functions selected, it is found sufficient to represent each of the annular zones by a single element.

4) The thermal expansion coefficients of the composite are obtained by computing the average strains over the volume V of the RVE for unit increase in temperature.

5) The properties of the composite element are taken to be those obtained at the end of the previous increment.

6) The residual thermal stresses are obtained by using the analytical approach described by Nairn.[23] The solution of the uniform thermal expansion of a three-phase composite cylinder has a form similar to that of the solution of a cylinder under internal and external pressure. Additional boundary conditions are supplied to ensure continuity at the interfaces of the three phases. This results in a set of linear simultaneous equations, which can be solved to compute the stress and strain fields in each of the phases. As a first guess, the initial thermal expansion coefficient of the composite material is obtained using a closed-form solution quoted by Yates et al.[24]

Details on the implementation of the FECM are given in Ref. 21.

Case Studies

General

To examine the accuracy of the proposed models, two case studies were undertaken. In each case, a characteristic stress–strain curve of a composite structure was obtained experimentally and then compared with predictions of nonlinear finite element analysis with material nonlinearities accounted for by the micromodels.

The first example consists of a V-notched (or Iosipescu) shear beam. The second example consists of 45/−45-deg cylinders with fixed ends subjected to axial compression. Details of each of the examples are given in subsequent sections.

Material Properties

The primary source of nonlinearity in these problems is that which comes from nonlinearity of the material response. The material properties of the ingredients of the systems studied are given in Tables 1 and 2. The properties of carbon fibers were obtained from product literature, and properties of matrix materials were obtained by testing neat epoxy samples in direct tension and Iosipescu shear tests. The Ramberg–Osgood material parameters of the epoxy (σ_o, n), were determined as the best-fit parameters to shear stress–strain curve, as obtained by the Iosipescu test. Typical shear and normal stress–strain responses of epoxy are shown in Fig. 6. Figure 6 gives both the experimentally obtained and curve-fitted responses of M337 epoxy. Here, α_1 and α_2 are coefficients of thermal expansion in the longitudinal and transverse direction of the fiber, and α_m is that of the matrix. The α are treated as constant in this study. All of the samples used were manufactured at Production Products, Inc., St. Louis, Missouri, and tested at the Structural Testing Laboratory in Washington University, St. Louis, Missouri.

Table 1 Carbon fiber properties

Material	E_1, GPa	E_2, GPa	ν_{12}	G_{12}, GPa	G_{23}, GPa	$\alpha_1/^\circ$ C	$\alpha_2/^\circ$C
Panex33 carbon fibers	228.0	26.2	0.31	24.8	9.8	-1×10^{-6}	8×10^{-6}
AS4 carbon fibers	234.4	16.5	0.31	24.8	6.2	-1×10^{-6}	8×10^{-6}

Table 2 Matrix properties

Material	E, GPa	ν	σ_0, MPa	n	σ_{ult}, MPa	α_m
M337 epoxy	3.95	0.26	188.2	2.58	57.5	60×10^{-6}
6010 epoxy	3.6	0.347	121.3	5.69	58.6	60×10^{-6}

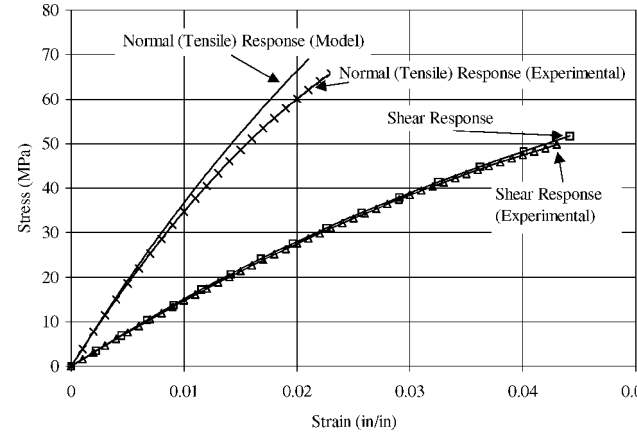

Fig. 6 Shear and normal response of M337 epoxy.

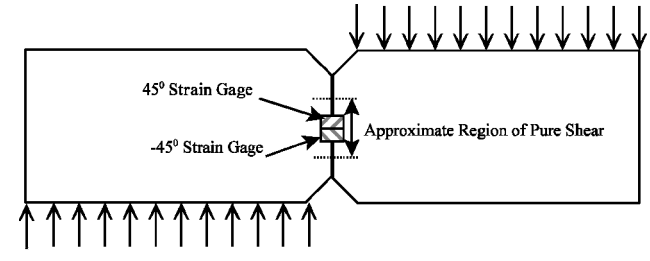

Fig. 7 Loading of the V-notched shear beam specimen.

V-Notched Shear Beams

Specimens and Details of Test Setup

The V-notched shear beam test specimen (Fig. 7) consists of a 76.2×19.05 mm (3×0.75 in.) coupon with two 3.81-mm (0.15-in.)-deep 90-deg V notches at the center. The symmetric specimen is subjected to antisymmetric load as shown in Fig. 7. Shear strains across the notched area were measured via a set of 45/−45-deg strain gauges placed on two faces of the specimen. Two

different material systems were tested: AS4/6010 and Panex33. The AS4/6010 samples were 3.81 mm (0.15 in.) thick, and the Panex33 samples were 3.66 mm (0.144 in., 12 layers) thick.

AS4/6010 Lamina

Test specimens were cut from the unidirectional panels of AS4/6010, which were manufactured via filament winding process using a box mandrel. The panels were cured at 180°F for 16 h and then allowed to cool down to room temperature (70°F). The specimens were so cut that fibers were oriented at 0 deg with respect to the length direction of the beam. (These specimens are referred to as lamina specimens.)

Panex33 Laminate

Cross-ply panels $[0/90]_{12}$ deg were made from Panex33 prepregs by hand layup and vacuum bagging. The panels were cured at 180°F for 16 h and then allowed to cool down to room temperature (70°F).

Modeling

The V-notched beams were analyzed using the scheme described earlier. The V-notched beam was discretized using eight-noded plane stress elements as shown in Fig. 8. Because of the geometric symmetry and antisymmetric loading, it is necessary to model only one-quarter of the beam. The nominal shear strain was obtained by averaging the values of the shear strains over the area covered by the gauge. The nominal stress is obtained by dividing the applied load by the cross-sectional area of the notch. Figure 9 shows a typical shear stress contour plot for a composite material using micromechanical analysis. It can be seen that the stress gradient in the strain gauge region is fairly small. The mesh shown in Fig. 8 was found to be sufficiently accurate after a mesh refinement study.

Results and Discussion

AS4/6010 Lamina

The experimental results and the model predictions are shown in Figs. 10–12. It can be seen from Fig. 10 that there are two noticeable discontinuities in the experimental response. They are associated with macrocracking of the lamina. As the specimen is loaded under shear, high-stress gradients develop at the root of the notch, leading to a visible crack that runs along the fibers. A sharp drop in the stress

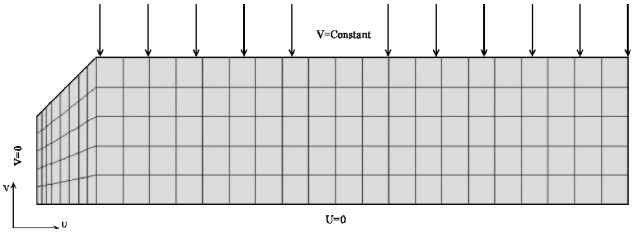

Fig. 8 ABAQUS model for notched beam specimen.

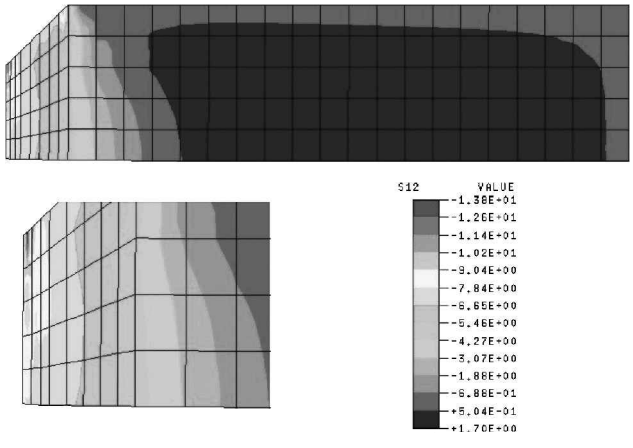

Fig. 9 Typical shear stress contours for 0-deg AS4/6010 specimen.

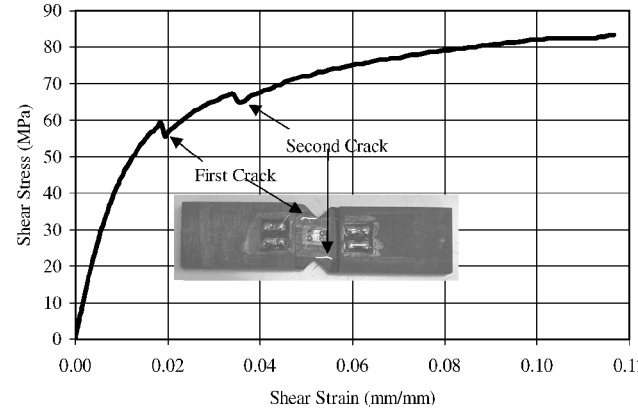

Fig. 10 Experimental response of 0-deg AS4/6010 specimens.

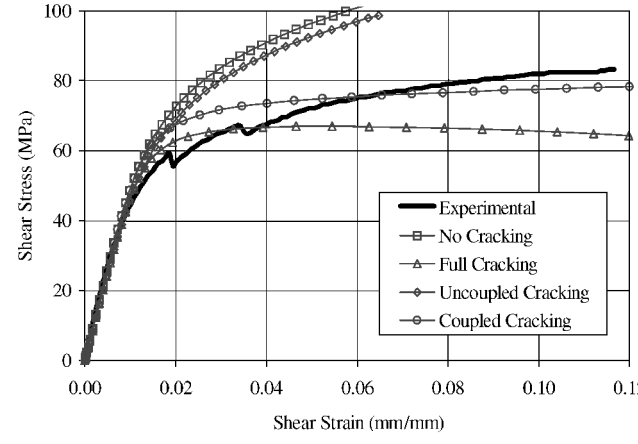

Fig. 11 FECM predictions of 0-deg AS4/6010 V-notched beam.

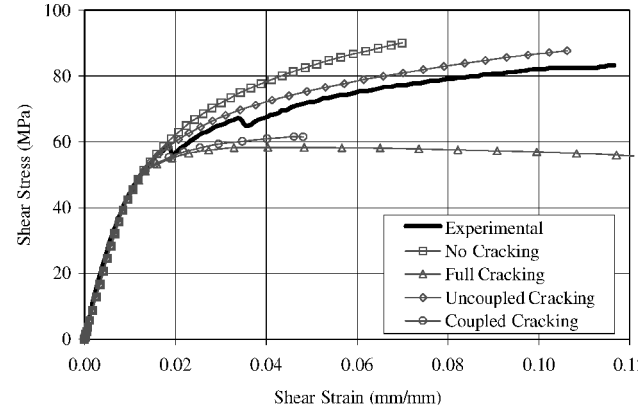

Fig. 12 SSCM predictions for 0-deg AS4/6010 specimen.

is seen when the crack nucleates and travels a small distance, where it gets locked. Typically, the first crack develops at the top notch, and then a second crack follows soon at the bottom notch. Such cracking is characteristic of notched laminas with fibers all running in 0 or 90 deg. The present model is not designed to deal with macrocracking emanating from a strong singularity because this calls for a fracture mechanics approach. However, the cracks were contained in a relatively small region, and the strain gauge readings are, therefore, believed to give values representative of average shear strain. Figure 11 shows the predictions of FECM. It can be seen that the closest response prediction is given by the coupled cracking option. For this case, FECM starts microcracking at a later stage than observed in the experiment. Furthermore, upon severe microcracking, the FECM response flattens out much faster than the experimental response. FECM, however, predicts the final stress level fairly well. The predictions of SSCM are shown in Fig. 12. The closest response

is given by the uncoupled cracking option. SSCM predicts earlier cracking than does FECM.

Panex33 Laminate

Unlike unidirectional laminas, these cross-ply laminates do not undergo macrocracking during testing, and the experimental curve for this case does not show any sudden drops as seen in case of AS4/6010 lamina. Figure 13 shows the experimental response with FECM predictions. It can be seen that FECM predicts the experimental response with great accuracy with the coupled cracking option. Figure 14 shows the predictions of SSCM. It can be seen that none of the cracking options provide a reasonably good estimate of the experimental response. This observation is consistent with the earlier observation[19] on the study of 45/−45-deg tension coupon, and as before, the failure of SSCM to predict the response correctly is linked to incorrect estimate of residual stresses, which stems from overly simplified way of computing micro-stresses in SSCM.

Compression Response of AS4/6010 Composite Cylinders

Specimen and Details of Test Setup

Filament-wound 45/−45-deg AS4/6010 cylinders were cured at 180°F for 16 h and then allowed to cool to room temperature (70°F). Two different thicknesses were used, namely, 2.3 mm (0.09 in.) and 4.7 mm (0.1865 in.). The fiber volume fractions were 0.538 and 0.513 for the thinner and thicker cylinders, respectively. The cylinders were tested under fixed-end conditions. The clear length between the fixtures was 101.6 mm (4 in.). The nominal axial stress is obtained by dividing the applied load by the cross-sectional area of the cylinder. Three 0/45/90-deg strain rosettes were placed on the outer face of each cylinder, 120-deg apart from each other, at the center of the cylinder. The nominal axial strain is obtained by averaging the axial strains obtained from the three strain gauges.

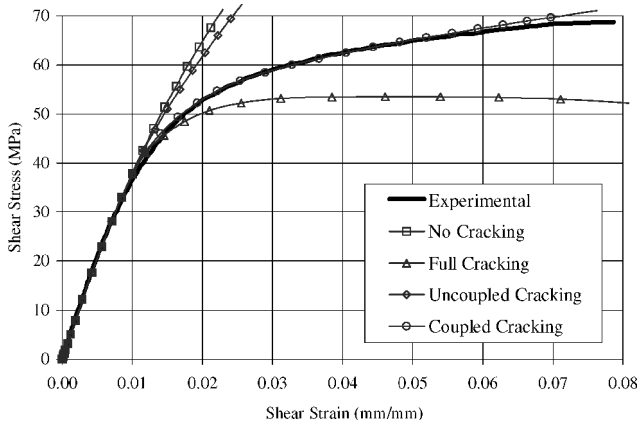

Fig. 13 Shear test on Panex33: experiment and FECM response.

Modeling

The micromechanics-based analysis of the cylinders was conducted using eight-noded axisymmetric solid elements (CGAX8 of ABAQUS). Because of the symmetric nature of the problem, it was necessary to model only half the length of the cylinder. Convergence studies were conducted by discretizing the cylinder using 5–10 elements in the axial direction and 2–4 elements in the thickness direction.[21] The coarsest mesh employed is shown in Fig. 15. To monitor material degradation, five integration points were used across the thickness per element. Typical deformed profile of the cylinder is shown in Fig. 16. Axial strain near the line of symmetry was compared with the strain gauge data.

Results and Discussion

Figures 17 and 18 show the SSCM and FECM predictions for the thin cylinder. Figures 19 and 20 show the SSCM and FECM predictions for the thick cylinder. It can be seen that SSCM is not able to predict the experimental response with any cracking option, although it does bound the results. FECM with coupled cracking option is closer to the experimental curve than with any other option. The level of ultimate stress taken by the cylinders before failure is predicted reasonably well by this option, although the curvature of the nonlinear response is not. Note that, even though the cylinders are under axial compression, there is a high level of tensile stresses induced in the hoop direction. These stresses cause microcracking in the composite. Figures 21 and 22 show typical contours of stresses in the axial and circumferential directions, respectively.

The FECM prediction of the cylinder behavior shows trends similar to those observed in its prediction of notched beam specimen, made of the same material and using the same filament winding process. The authors believe that this discrepancy is due to process-induced effects associated with filament winding, such as the stresses induced and the nonuniformity of the fiber-volume fraction. Further studies are needed to understand the discrepancy in the predictions of FECM for the filament-wound composite specimens.

Influence of Residual Stresses

It is of interest to study the effect of the residual stresses and to what extent they have modified the predictions.

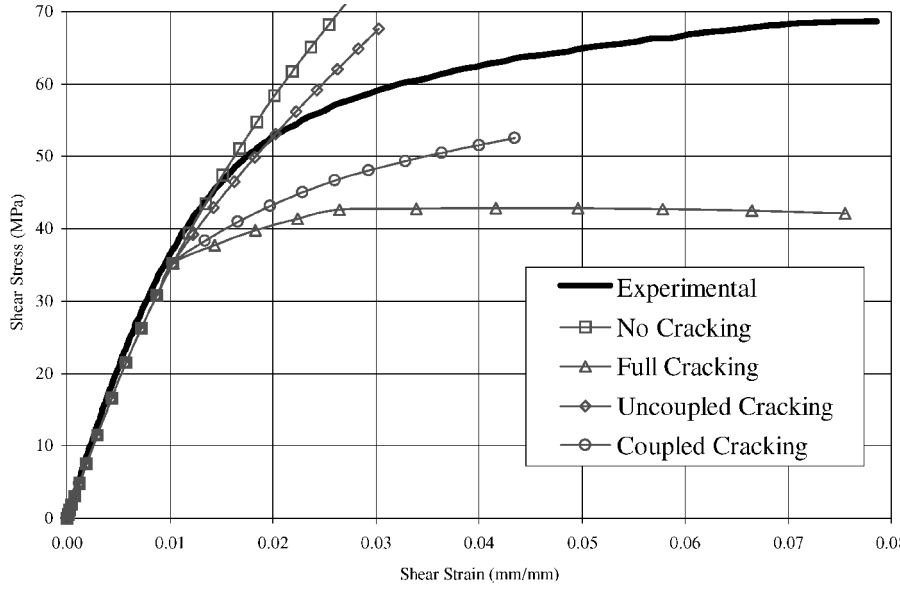

Fig. 14 Shear test on Panex33: experiment and SSCM response.

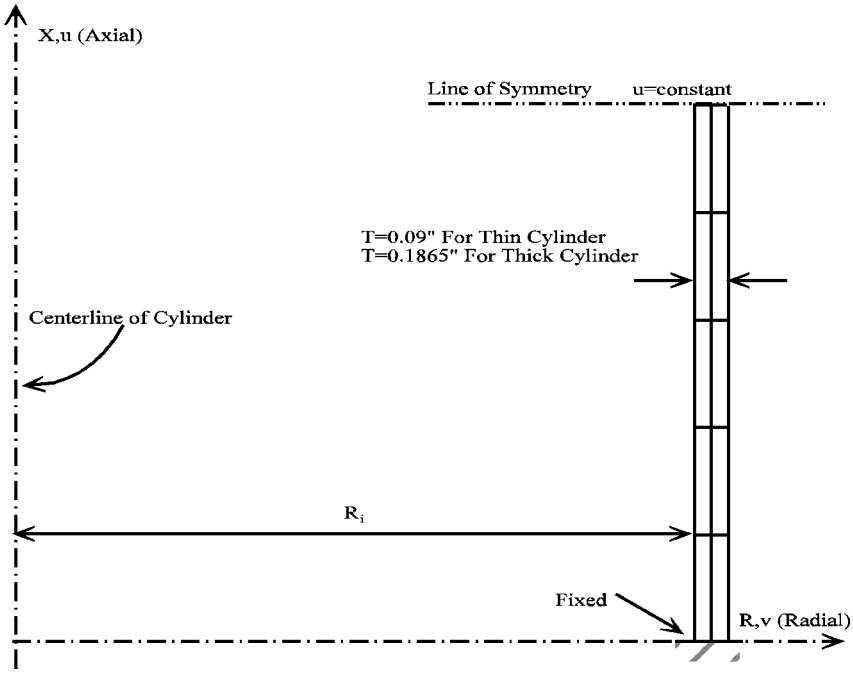

Fig. 15 Cylinder geometry and discretization.

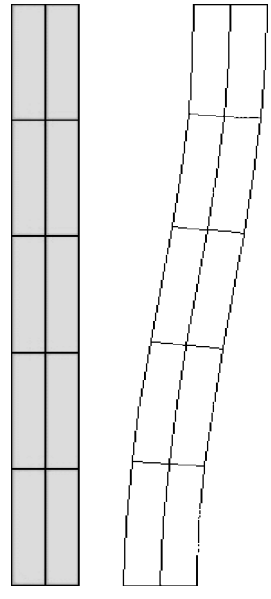

Fig. 16 Undeformed and deformed profiles.

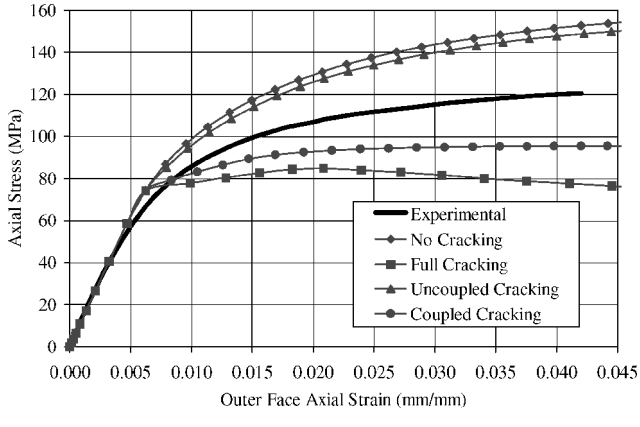

Fig. 17 SSCM prediction of thin cylinder response.

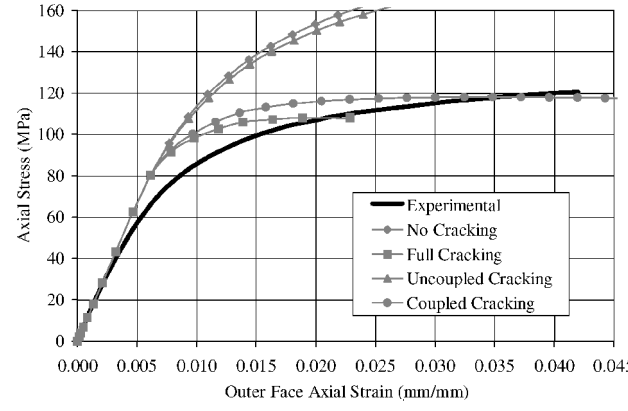

Fig. 18 FECM prediction of thin cylinder response.

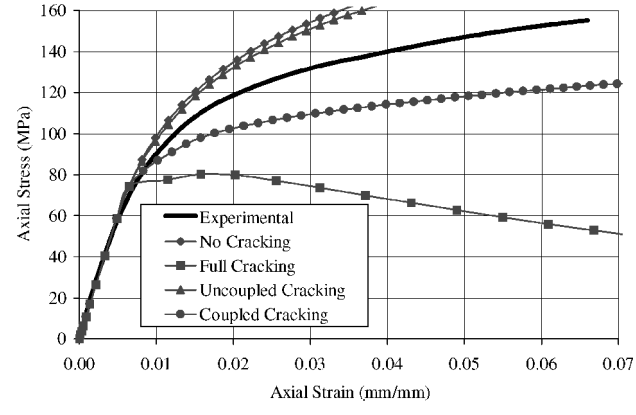

Fig. 19 SSCM prediction of thick cylinder response.

Figure 23 shows the predictions of axial stress–strain response of the thicker cylinder as given by FECM with the coupled cracking option. Of the two predictions shown, the higher result was obtained by neglecting the residual stresses, whereas the other was obtained duly including the same. Figure 23 shows the corresponding experimental result as well. The two model predictions part company at an early stage in the loading history, but run roughly parallel to each other in the advanced stages, where the two models differ by about 30% in their prediction of the load-carrying capacity.

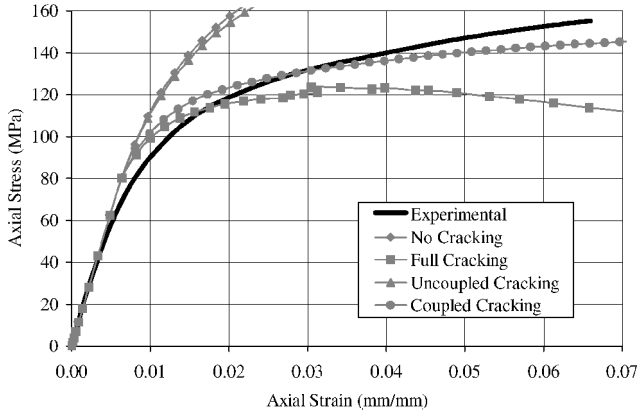

Fig. 20 FECM prediction of thick cylinder response.

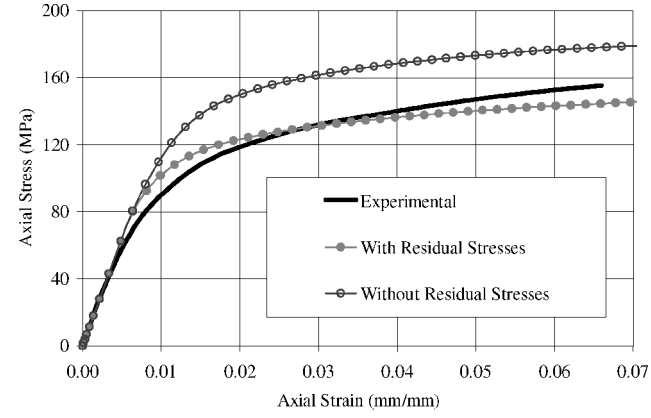

Fig. 23 Effect of residual stresses on FECM predictions (coupled cracking).

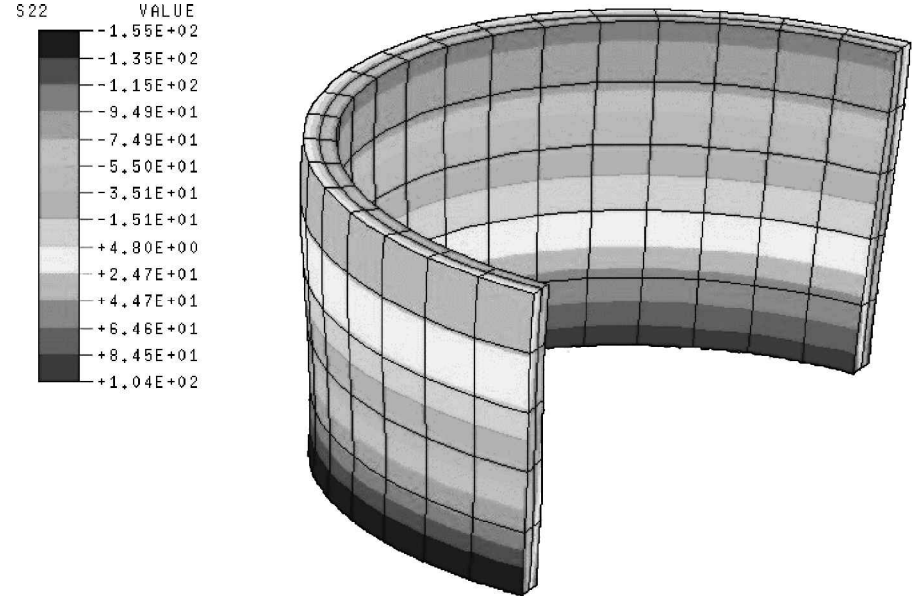

Fig. 21 Typical axial stress contours for AS4/6010 cylinders.

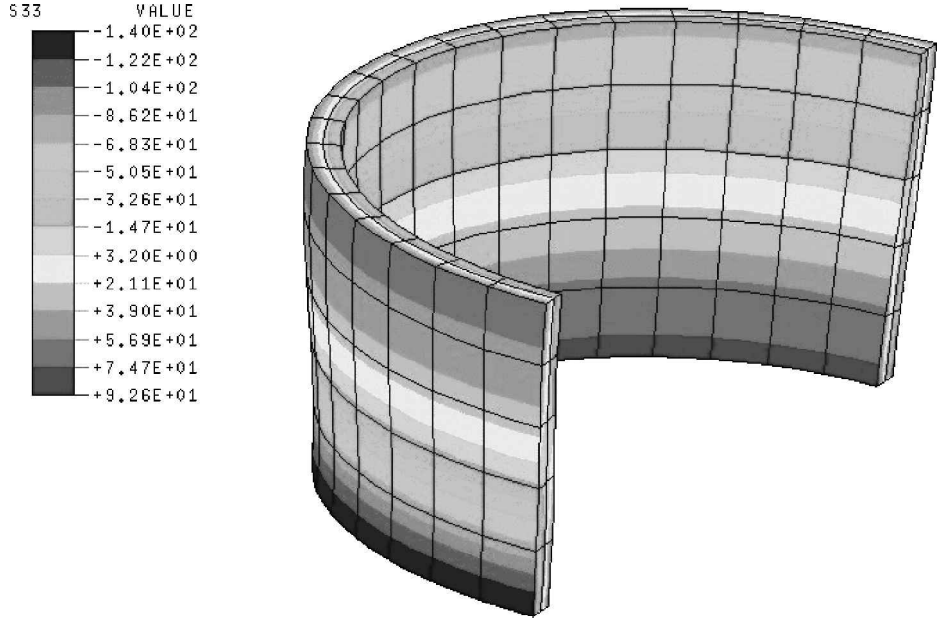

Fig. 22 Typical transverse stress contours for AS4/6010 cylinders.

Conclusions

Micromodels based on square cells (SSCM) and cylindrical cells (FECM) were developed using actual properties (as against tuned properties) of the matrix and explicitly accounting for residual stresses and microcracking. These models were interfaced with a nonlinear finite element analysis program for performing nonlinear analysis of composite structures. Two types of structural elements were investigated with a view to assess the viability of the use of such models for practical structural analysis and the accuracy with which nonlinear response is predicted. These are V-notched shear beam specimens and 45/−45-deg cylinders. The conclusions gleaned from the studies are summarized as follows:

1) FECM with the coupled cracking option was able to predict the nonlinear response of laminates in general. This was seen in the case of notched Panex33 laminate in shear as well as 45/−45-deg cylindrical shells under axial compression. The authors believe that the coupledcracking option mimics the actual cracking behavior more realistically than other options. However, more experimental studies are needed to confirm this hypothesis.

2) SSCM, in general, did not produce results of consistent accuracy. One exception is the case of AS4/6010 lamina in shear, whose response was captured using the uncoupled cracking option. However, the model could not capture any of the other test results with reasonable accuracy.

3) There was clearly some discrepancy in the FECM predictions and the response of specimen manufactured using the filament winding process. Even though the maximum load was predicted with fair accuracy, the curvature of the stress–strain response was not well predicted. Further studies are needed to understand why this occurs and to correct for any process-induced effects associated with the filament winding process.

4) Residual stresses play a significant role, and their inclusion is crucial to obtaining reliable predictions of the maximum load. SSCM model does a poor job of predicting the residual stresses, and this is believed to be a factor in its poor performance.

Acknowledgments

The study was supported by Office of Naval Research Grant N00014-J-91-1637(Scientific Program Officer, Y. D. S. Rajapakse) and by a Boeing Foundation Fellowship (Boeing Contact, M. J. Johnson).

References

[1]Aboudi, J., *Mechanics of Composite Materials: Unified Micro-Mechanical Approach*, Elsevier, New York, 1991.

[2]Robertson, D. D., and Mall, S., "Micro-Mechanical Relations for Fiber-Reinforced Composites Using Free Transverse Shear Approach," *Journal of Composites Technology and Research*, Vol. 15, No. 3, 1993, pp. 181–192.

[3]Hill, R., "Elastic Properties of Reinforced Solids: Some Theoretical Principles," *Journal of Mechanics and Physics of Solids*, Vol. 11, 1963, pp. 357–372.

[4]Hashin, Z., and Rosen, B. W., "The Elastic Moduli of Fiber-Reinforced Materials," *Journal of Applied Mechanics*, Vol. 31, 1964, pp. 223–232.

[5]Chamis, C. C., and Sendeckyj, G. P., "Critique on Theories Predicting Thermoelastic Properties of Fibrous Composites," *Journal of Composite Materials,* Vol. 2, No. 3, 1968, pp. 332–358.

[6]Hashin, Z., "Analysis of Composite Materials—A Survey," *Journal of Applied Mechanics*, Vol. 50, 1983, pp. 481–505.

[7]Lissenden, C. J., and Herakovich, C. T., "Comparison of Micro-Mechanical Models for Elastic Properties," *SPACE'92, Proceedings of the Third International Conference*, ASCE, New York, 1992, pp. 1309–1322.

[8]Rahman, S., and Pecknold, D. A., "Micromechanics Based Analysis of Fiber-Reinforced Laminated Composites, Dept. of Civil Engineering, Rept. UILU-ENG-92-2012, Univ. of Illinois, Urbana, Il, Sept. 1992.

[9]Jones, R. M., *Mechanics of Composite Materials*, Hemisphere, New York, 1998, Chap. 3.

[10]Aboudi, J., "The Nonlinear Behavior of Unidirectional and Laminated Composites–A Micro-Mechanical Approach," *Journal of Reinforced Plastics and Composites,* Vol. 29, 1990, pp. 13–32.

[11]Arenberg, R. T., "Analysis of Metal Matrix Composite Structures Using a Micro-Mechanical Constitutive Theory," Ph.D. Dissertation, Dept. of Mechanical Engineering, Virginia Polytechnic Inst. and State Univ., Blacksburg, VA, 1988.

[12]Robertson, D. D., and Mall, S., "Micro-Mechanical Analysis of Metal Matrix Composite Laminates with Fiber/Matrix Interfacial Damage," *Composites Engineering*, Vol. 4, No. 12, 1994, pp. 1257–1274.

[13]Robertson, D. D., and Mall, S., "Incorporating Fiber Damage in a Micro-Mechanical Analysis of Metal Matrix Composite Laminates," *Journal of Composites Technology and Research*, Vol. 18, No. 4, 1996, pp. 265–273.

[14]Gates, T. S., Chen, J. L., and Sun, C. T., "Micro-Mechanical Characterization of Nonlinear Behavior of Advanced Polymer Matrix Composites," *Composite Materials: Testing and Design (Twelfth Volume)*, ASTM STP 1274, edited by R. B. Deo and C. R. Saff, American Society for Testing and Materials, Philadelphia, 1996, pp. 295–319.

[15]Sun, C. T., and Chen, J. L., "A Micro-Mechanical Model for Plastic Behavior of Fibrous Composites," *Composites Science and Technology*, Vol. 40, 1991, pp. 115–129.

[16]Pecknold, D. A., and Haj, Ali R., "Integrated Micro-Mechanical/ Structural Analysis of Laminated Composites," *Mechanics of Composite Materials; Nonlinear Effects*, AMD-Vol. 159, American Society of Mechanical Engineers, Fairfield, NJ, 1993, pp. 197–206.

[17]Pecknold, D. A., and Rahman, S., "Application of a New Micro-Mechanics-Based Homogenization Technique for Nonlinear Compression of Thick-Section Laminates," *Compression Response of Composite Structures*, edited by S. E. Groves and A. L. Highsmith, ASTM STP 1185, American Society for Testing and Materials, Philadelphia, 1994, pp. 34–54.

[18]Jadhav,V. R., and Sridharan, S., "A Comparative Study of Micromodels for Nonlinear Analysis of laminas," *Journal of Composite Materials*, Vol. 33, No. 18, 1999, pp. 1666–1684.

[19]Jadhav, V. R., and Sridharan, S., "Micro-Mechanical Modeling of Polymer Based Unidirectional Composites: Use of Bulk Properties of Matrix with the Smeared Crack Model," *Journal of Composite Materials*, Vol. 36, No. 24, 2002, pp. 2735–2763.

[20]"ABAQUS/Standard User's Manual," Ver. 5.8, Vol. 1–3, Hibbit, Karlsson, and Sorensen, Inc., Pawtucket, RI, 1998.

[21]Jadhav, V. R., "Micro-Mechanical Analysis of Unidirectional Composites," D.Sc. Dissertation, Washington Univ., St. Louis, MO, Dec. 2000.

[22]Rots, J. G., "Crack Models for Concrete: Discrete or Smeared? Fixed, Multi-Directional or Rotating?," *Heron*, Vol. 34, No. 1, 1989, pp. 1–58.

[23]Nairn, J. A., "Thermoelastic Analysis of Residual Stresses in Unidirectional High-Performance Composites," *Polymer Composites*, Vol. 6, No. 2, 1985, pp. 123–130.

[24]Yates, B., Overy, M. J., Sargent, J. P., McGalla, B. A., Kingston-Lee, D. M., Phillips, L. N., and Rogers, K. F.,"Thermal Expansion of Carbon Fibre-Reinforced Plastics," *Journal of Materials Science*, Vol. 13, 1978, pp. 433–440.

K. N. Shivakumar
Associate Editor